AGU PUBLICATIONS

Journal of Advances in Modeling Earth Systems

RESEARCH ARTICLE
10.1002/2016MS000670

Key Points:
- ACRE simultaneously enhances and reduces high cloud amount through two different physical mechanisms.
- High cloud reduction through indirect cloud heating dominates the cloud response in limited-domain experiments
- ACRE produces more high, optically thin clouds relative to high, optically thick clouds, and thus increases TOA CRE

Correspondence to:
B. E. Harrop,
beharrop@u.washington.edu

Citation:
Harrop, B. E., and D. L. Hartmann (2016), The role of cloud radiative heating within the atmosphere on the high cloud amount and top-of-atmosphere cloud radiative effect, *J. Adv. Model. Earth Syst.*, *8*, doi:10.1002/2016MS000670.

Received 9 MAR 2016
Accepted 2 AUG 2016
Accepted article online 5 AUG 2016

© 2016. The Authors.
This is an open access article under the terms of the Creative Commons Attribution-NonCommercial-NoDerivs License, which permits use and distribution in any medium, provided the original work is properly cited, the use is non-commercial and no modifications or adaptations are made.

The role of cloud radiative heating within the atmosphere on the high cloud amount and top-of-atmosphere cloud radiative effect

Bryce E. Harrop[1] and Dennis L. Hartmann[1]

[1]Department of Atmospheric Sciences, University of Washington, Seattle, Washington, USA

Abstract The effect of cloud-radiation interactions on cloud properties is examined in the context of a limited-domain cloud-resolving model. The atmospheric cloud radiative effect (ACRE) influences the areal extent of tropical high clouds in two distinct ways. The first is through direct radiative destabilization of the elevated cloud layers, mostly as a result of longwave radiation heating the cloud bottom and cooling the cloud top. The second effect is radiative stabilization, whereby cloud radiative heating of the atmospheric column stabilizes the atmosphere to deep convection. In limited area domain simulations, the stabilizing (or indirect) effect is the dominant role of the cloud radiative heating, thus reducing the cloud cover in simulations where ACRE is included compared to those where it is removed. Direct cloud radiative heating increases high cloud fraction, decreases mean cloud optical depth, and increases cloud top temperature. The indirect cloud radiative heating decreases high cloud fraction, but also decreases mean cloud optical depth and increases cloud top temperature. The combination of these effects increases the top-of-atmosphere cloud radiative effect. In mock-Walker circulation experiments, the decrease in high cloud amount owing to radiative stabilization tends to cancel out the increase in high cloud amount owing to the destabilization within the cloud layer. The changes in cloud optical depth and cloud top pressure, however, are similar to those produced in the limited area domain simulations.

1. Introduction

Clouds have a strong impact on the radiative budget of the atmosphere. They influence the amount of shortwave and longwave radiation absorbed by the atmosphere and surface. The effect of clouds on the energy balance of the atmosphere is quite different from their effect at the surface or the top of the atmosphere. On average, clouds cool the surface by reflecting shortwave radiation, and may heat it by increasing the downward flux of longwave radiation. The effect of clouds on the atmospheric energy budget, however, is less straightforward. Because the tropospheric lapse rate is positive, clouds can either warm or cool the atmosphere, depending on their vertical structure. Low clouds can cool the atmosphere by increasing the downward emission of longwave radiation, while high clouds warm it by decreasing the upward emission of longwave radiation [see, e.g., *Slingo and Slingo*, 1988]. Over regions of deep convection within the tropics where high clouds dominate, cloud-radiation interactions warm the upper troposphere because absorption of longwave and shortwave radiation is much larger than the cloudy emission of longwave radiation [*Slingo and Slingo*, 1988].

The cloud radiative heating within the atmosphere (the difference in the all-sky and clear-sky radiative heating profiles) is termed the atmospheric cloud radiative effect (ACRE). ACRE is similar to the often discussed top-of-atmosphere cloud radiative effect (CRE) because both contrast radiative fluxes with and without clouds. CRE describes the change in radiant flux through the top of the atmosphere owing to clouds, while ACRE describe the change in radiative heating within the atmosphere owing to clouds. It has been shown that including a realistic profile of ACRE within a model drives more realistic tropical circulations [*Hartmann et al*., 1984; *Tian and Ramanathan*, 2003]. It has also been shown that ACRE feeds back on the clouds through destabilization of the cloud layer by radiation [*Webster and Stephens*, 1980; *Ackerman et al*., 1988; *Chen and Cotton*, 1988; *Lilly*, 1988; *Fu et al*., 1995; *Mace et al*., 2006]. We will refer to this destabilization of the cloud layer by radiation as the "direct effect of ACRE," or "direct effect" for short. *Webster and Stephens* [1980] calculated the heating gradient in thick anvil clouds near the West Pacific warm pool to be up to 35 K/d between cloud bottom and top, while *Ackerman et al*. [1988] later showed that the heating profile of

anvil clouds can vary by as much as 200 K/d from the bottom to the top of the anvil cloud. *Powell et al*. [2012] showed that the heating and cooling at cloud bottom and top, respectively, is greatest for the thickest anvils. *Fu et al*. [1995] showed that a simulated squall line system run with interactive cloud radiation produced greater high cloud cover than the same squall line system run without interactive cloud radiation. They also noted, however, that the cloud radiative heating would begin to stabilize the atmosphere to deep convection if they continued their experiments beyond a few hours. Similar cloud expansion can be simulated for tropical tropopause layer cirrus as shown by *Durran et al*. [2009] and *Dinh et al*. [2010].

As already noted, ACRE is positive in tropical convective regions [*Slingo and Slingo*, 1988], and thus, the upper troposphere is warmed by radiative heating within the clouds [see also, *Slingo and Slingo*, 1991]. We will refer to this heating of the upper troposphere as the "indirect effect of ACRE" or "indirect effect" for short. *Sherwood et al*. [1994] found that removing the cloud-radiation interactions in a general circulation model reduced the cloud cover over the tropical warm pool. It is unlikely, however, that their model setup was capable of resolving the within-cloud destabilization process, and it is unclear whether the radiative heating gradient between cloud bottom and top would sustain clouds without this mixing. Thus it is difficult to assess the relative importance of both the cloud-layer destabilization (the direct effect) and the atmospheric stability change (the indirect effect) from the *Sherwood et al*. [1994] experiments.

Lebsock et al. [2010] showed a strong correlation between tropical mean convection and cloud radiative fields on daily timescales. They showed that tropical mean precipitation correlates positively with reflected shortwave and negatively with outgoing longwave radiation. They suggested a "radiative-convective cloud feedback," wherein precipitation enhances clouds, which decrease the radiative cooling, and hence reduce precipitation. In this paper, we include an additional pathway in which the radiation changes associated with clouds feeds back on the clouds directly.

To summarize, cloud-radiation interactions have been shown to be important for destabilizing anvil clouds in tropical deep convective systems (the direct effect). It has also been suggested that the net heating of the upper troposphere by these clouds will stabilize the atmosphere to deep convection (the indirect effect), which will change other components of the tropical system such as the OLR and the precipitation. Much of the prior work centers on case studies of individual cloud systems and their interaction with radiation [e.g., *Fu et al*., 1995; *Durran et al*., 2009; *Dinh et al*., 2010]. Other studies have examined the change in cloud amount to the heating of the atmosphere by ACRE [e.g., *Sherwood et al*., 1994]. To our knowledge, however, ours is the first study to examine both of these effects together to quantify the net impact of cloud-radiation interactions on the tropical clouds.

We have designed a series of equilibrium cloud-resolving model experiments as a means of exploring this problem, and with which we can examine the role of cloud radiative heating on tropical convection. Equilibrium experiments allow us to collect statistics from numerous cloud life cycles instead of relying on a single cloud system from which to draw conclusions. We hope to address several questions in this paper: (1) how does cloud fraction respond to ACRE? (2) How does the top-of-atmosphere cloud radiative effect respond to ACRE? (3) Does a large-scale circulation mitigate the stability effect of the cloud radiative heating? and (4) What are the implications for cloud feedbacks?

In this paper, we confirm that the cloud fraction increases owing to an increase in turbulent kinetic energy driven by direct cloud-radiation interactions. We also show, however, that the indirect stability changes over the depth of the troposphere dominate the cloud fraction by stabilizing the atmosphere to deep convection and limiting both the cloud fraction and the precipitation. We show that the total (direct + indirect) cloud radiative heating further changes the clouds to be both thinner and warmer, making the top-of-atmosphere cloud radiative effect (CRE) less negative. We also show that the indirect stability effect is mitigated somewhat by having a large-scale circulation within the model that can transport energy to a region where it can be radiated to space more efficiently. Finally, current general circulation models predict a reduction in high cloud amount [see, e.g., *Zelinka et al*., 2012], and we suggest this reduction may be exaggerated owing to these models' inability to resolve within-cloud circulations.

2. Model Details and Experimental Design

We use the System for Atmospheric Modeling (SAM) cloud-resolving model version 6.7 [*Khairoutdinov and Randall*, 2003]. The model uses the anelastic equations of motion, has a rigid lid at roughly 40 km, and

Newtonian damping in the upper third. It has three prognostic variables: liquid water/ice moist static energy, total nonprecipitating water (vapor, cloud liquid, and cloud ice), and total precipitating water (rain, snow, and graupel). The vertical grid is stretched with 96 levels. The vertical grid spacing varies from less than 100 m in the boundary layer, to roughly 300 m in the upper troposphere, and finally to 1 km spacing in the stratosphere. The simulations are run with doubly periodic boundary conditions on the sides and fixed SST (either uniform or sinusoidal as we will discuss later). Monin-Obukhov similarity is used to compute the surface turbulent fluxes. Diffusion is handled with a 1.5-order closure scheme based on subgrid scale turbulent kinetic energy and also incorporates a simple Smagorinsky-type scheme. There is no artificial diffusion added. The Rapid and Accurate Radiative Transfer Model for GCMs is used for the radiative transfer calculations [see *Mlawer et al*., 1997; *Iacono et al*., 2008]. The simulations are performed at the equator with no rotation and perpetual insolation. The zenith angle for insolation is set as the daily average value. We follow the work of *Harrop and Hartmann* [2012] for determining when the model has reached radiative convective equilibrium (the model is in equilibrium when the net heating of the atmosphere is approximately zero). In their study, 50 days were used for model spin up. We allow 50 days of model spin up for our small domain experiments as well. We find that while some of the integrations reach equilibration prior to day 50, all of the integrations are in equilibrium by day 50. For the mock-Walker circulation experiments, not all of the simulations were equilibrated by day 50, but were by day 70. After equilibration, 50 additional days of simulation were run to collect statistics (for the small-domain experiments, days 50–100; for the mock-Walker experiments, days 70–120).

We first perform a suite of simulations with a horizontal grid of 96 km $\times$ 96 km with 1 km grid spacing. In these small-domain simulations, we use a uniform fixed sea surface temperature for the lower boundary condition. The 96 $\times$ 96 small domain was selected based on prior work [*Harrop and Hartmann*, 2012] to avoid self-aggregation occurring within the model. Cloud radiative effects have been shown to be an important component of the self-aggregation process [*Bretherton et al*., 2005; *Muller and Held*, 2012; *Wing and Emanuel*, 2014; *Muller and Bony*, 2015]. Since our experiments involve removing the cloud-radiation interactions, we expect that removing ACRE will cause disaggregation, thus convolving ACRE effects with aggregation effects. We have verified that convection is not aggregated in the small-domain experiments with the ratio of the driest to wettest quartile of column-integrated water vapor [following *Bretherton et al*., 2005]. The ratio of driest to wettest quartile is above 0.95 for all of the small-domain experiments (see Table 2). In the real tropical warm pool, energy is diverged through atmospheric motions that are not present in these small-domain simulations. Thus, we perform a similar set of simulations within a mock-Walker experiment. The mock-Walker simulations are run on a 6144 km $\times$ 32 km domain with 4 km grid spacing. We tested the sensitivity of the cloud areal extent and ACRE profiles to resolution in the small domain and found little change between 1, 2, 3, or 4 km horizontal grid spacings, so we do not expect the change from 1 to 4 km horizontal grid spacing to be a major difference between the two modeling setups. For the mock-Walker simulations, the sea surface temperature (SST) is again held fixed, but in these experiments, we introduce a sinusoidal SST pattern with a peak-to-peak amplitude of 4 K. 4 K is roughly the difference in sea surface temperature difference between the center and edge of the warm pool. Since our model only extends 6144 km, the gradient in SST is steeper than what is observed. The gradient in our model was chosen to match that used by *Wofsy and Kuang* [2012], in which they produced a reasonable Walker-like circulation.

We run the model both with the cloud-radiation interactions included (T1C1) and with the cloud-radiation interactions removed (T0C0). We will explain our notation in greater detail later, but "T" stands for experiments where ACRE heats the troposphere (the indirect effect) and "C" stands for experiments where ACRE heats the cloud layers (the direct effect). When the cloud-radiation interactions are removed, the clear-sky radiative heating rates are used to update the energy tendency terms, making the clouds invisible to both shortwave and longwave radiation. To separate the cloud changes associated with the direct radiative heating of clouds from those associated with the stability (indirect) effect, we run another pair of simulations. In the first, we still use the clear-sky fluxes to update the energy budget, but we additionally add in the domain mean average ACRE from the T1C1 experiment. In this case, the domain mean radiative cooling profile remains the same between this experiment and the T1C1 experiment, but the direct cloud-radiation interactions are removed, so that only the indirect effect is included. We refer to this experiment as T1C0. For the T1C0 experiments, the radiative heating rate is computed as follows:

$$Q_{\mathrm{RAD}}(i,j,k) = Q_{\mathrm{RAD,CLR}}(i,j,k) + \overline{[\mathrm{ACRE}]}_{\mathrm{T1C1}}(k), \quad (1)$$

where Q_{RAD} is the radiative heating rate, $Q_{\mathrm{RAD,CLR}}$ is the clear-sky radiative heating, and $\overline{[\mathrm{ACRE}]}_{\mathrm{T1C1}}$ is the domain mean, time-average ACRE profile from the T1C1 experiment (with the same domain size and SST as the T1C0 experiment). Square brackets indicate the domain mean and overbar denotes a time mean.

In the second experiment, ACRE is included, but we remove its domain mean profile at each time step. Again, this method has the desired effect of maintaining a radiative cooling profile that matches that of the T0C0 experiment, but still allows for the radiative heating within the clouds to occur. We refer to this experiment as T0C1. For the T0C1 experiments, the radiative heating rate is computed as follows:

$$Q_{\mathrm{RAD}}(i,j,k) = Q_{\mathrm{RAD,ALL}}(i,j,k) - [\mathrm{ACRE}]_{\mathrm{T0C1}}(k), \quad (2)$$

where $Q_{\mathrm{RAD,ALL}}$ is the all-sky radiative heating rate and $[\mathrm{ACRE}]_{\mathrm{T0C1}}$ is the domain mean ACRE for the T0C1 experiment. In other words, each time the radiation is called (every 160 s in our simulations) the domain mean ACRE value is removed from each column. Thus, the radiative heating gradients associated with the clouds are preserved, hence the C1 notation, while the domain mean ACRE is still zero at every time step, hence T0. The distribution of cloud bases (defined as the lowest level where ice cloud exists $q_i > 10^{-5}$ kg/kg) occupies a broad range from roughly 7 to 15 km (not shown). Longwave flux convergence dominates ACRE and is largest at cloud base. As a result, the mean ACRE profile is the result of averaging clouds at different levels, and therefore removing the mean profile should not noticeably diminish the strength of the within-cloud circulations (the direct effect) in our T0C1 experiments.

These four experiments allow us to examine the direct effect of ACRE on the clouds by differencing the T1C1 and T1C0 as well as the T0C1 and T0C0 experiments. Similarly, we can investigate the indirect effect of ACRE stabilizing the atmosphere and thus suppressing deep convection by differencing the T1C1 and T0C1 experiments or the T1C0 and T0C0 experiments. The experimental design is summarized in Figure 1, including the separation of the direct and indirect effects of ACRE on the cloud heating and tropospheric radiative heating profiles. Another separation that could be contemplated is the extent to which the ACRE results in a temperature change as opposed to a circulation change. This depends on the scale of the clouds and the domain with which they interact. By comparing the small domain and mock-Walker experiments, we can explore this separation. In the small domain, more of the effect of ACRE results in a temperature change, or the indirect effect. In the mock-Walker example, a larger fraction of the ACRE is exported away from the cloud by a circulation. Other factors such as self-aggregation or water vapor likely also have the effect of changing the relative roles of temperature change versus circulation change, and should be explored in future work.

In the limited area domain simulations, the T1C0 and T0C1 experiments have the advantage that they preserve the domain mean integrated radiative cooling and surface precipitation of their T1C1 and T0C0 counterparts, respectively. In the mock-Walker circulation experiments, however, the precipitation is not conserved because adding/removing the domain mean-ACRE uniformly across the domain does not preserve the structure in the time-average radiative cooling distribution, so the large-scale circulation will adjust.

The single moment microphysics scheme in SAM does not produce a lot of high, thin clouds, which makes the ACRE signal small in this modeling framework. To amplify the signal, we make use of a modification to the microphysics scheme based on the work of *Lopez et al*. [2009], which produces more realistic anvil cloud, tuned to reproduce tropical high cloud optical depth statistics observed by MODIS. We employ their "NOSEDAALIQ5" specifications, which remove cloud ice sedimentation, lower the threshold for ice autoconversion by a factor of 100, and increase the autoconversion and accretion of liquid by factors of five. For convenience, we will refer to this perturbed scheme as the "NA5" microphysics. The NA5 microphysics produces more extensive anvil and cirrus clouds within the model, enhancing the ACRE profile within our simulations. As a result, the NA5 microphysics does a much better job of reproducing a realistic ACRE heating profile (see Figure 2) compared to cloud heating rates calculated using CloudSat/CALIPSO/MODIS retrievals over the tropical warm pool (heating rate data provided by Qiang Fu). For the upper troposphere in the NA5 version of the model, the longwave heating is a little too strong compared to observations, while the shortwave heating is a little too weak, such that the net is nearly identical to observations. The model does not generate sufficient midlevel clouds, so it is missing the additional peak near 6 km. A horizontal

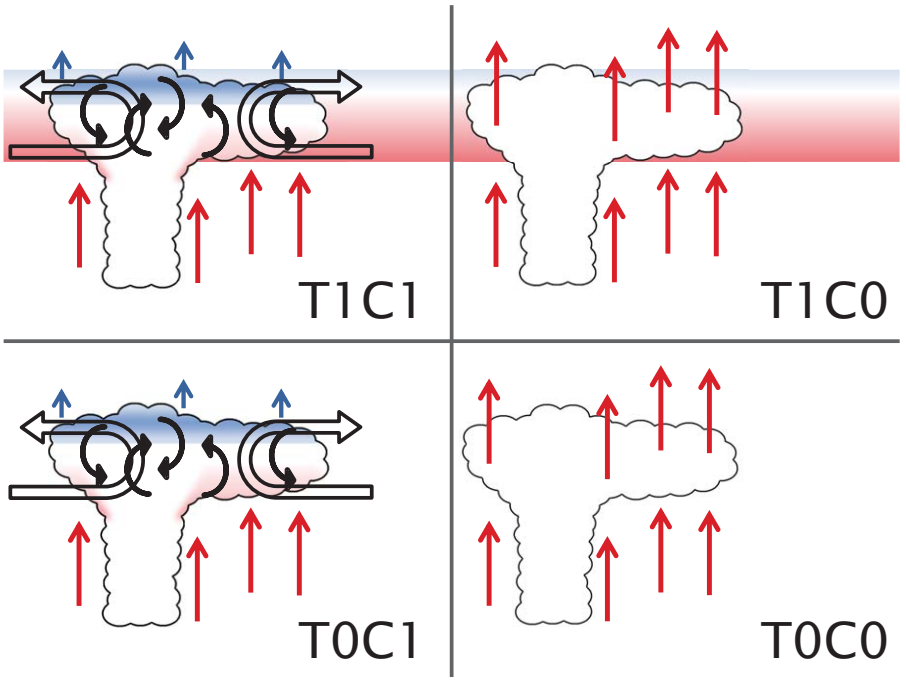


Figure 1. Schematic description of experiments. Red arrows are longwave emissions from the lower troposphere, blue arrows are longwave emissions at cloud top, black arrows denote circulations within the cloud, shading within cloud shows heating (red) and cooling (blue), shading outside of cloud shows the time-average, domain mean heating by clouds on the troposphere. (a) Control setup (T1C1); clouds interact with radiation to create circulations within the cloud (direct effect) and heating of the upper troposphere (indirect effect). (b) T1C0 experiment; clouds are invisible to radiation call, but time-average, domain-mean ACRE profile is added to the tropospheric heating. (c) T0C1 experiment; clouds interact with radiation as in T1C1, but at each time step the domain-mean ACRE is removed from the profile. (d) T0C0 experiment; clouds are invisible to radiation. The schematic illustrates the role of longwave, which is the dominant factor, but the shortwave heating by clouds is treated the same way as longwave in terms of its impact on the direct and indirect effects within the simulations. The within-cloud circulations depicted in the two "C1" experiments show both turbulent motions and a coherent circulation between the cloudy and clear-sky. We expect the coherent circulation is more likely to be occurring based off the work of *Durran et al.* [2009] and *Dinh et al.* [2010]. While we do not determine the relative strength of these circulation types in our simulations, we note that both are consistent with the increase in cloud amount we show in our results.

grid spacing of 1 km is insufficient for resolving low clouds accurately [*Bretherton et al.*, 2006], so we do not expect to accurately reproduce the heating rates in the lowest part of the atmosphere.

We run the NA5 microphysics for the T1C1, T0C0, T1C0, and T0C1 configurations at sea surface temperatures of both 28.5°C and 32.5°C for the uniform SST experiments. We also run two different SST profiles for the mock-Walker experiments. In the first, the peak temperature in the warm pool is 28.5°C, and in the second, the peak temperature is 32.5°C. For reference, the West Pacific warm pool sea surface temperatures are near 30°C.

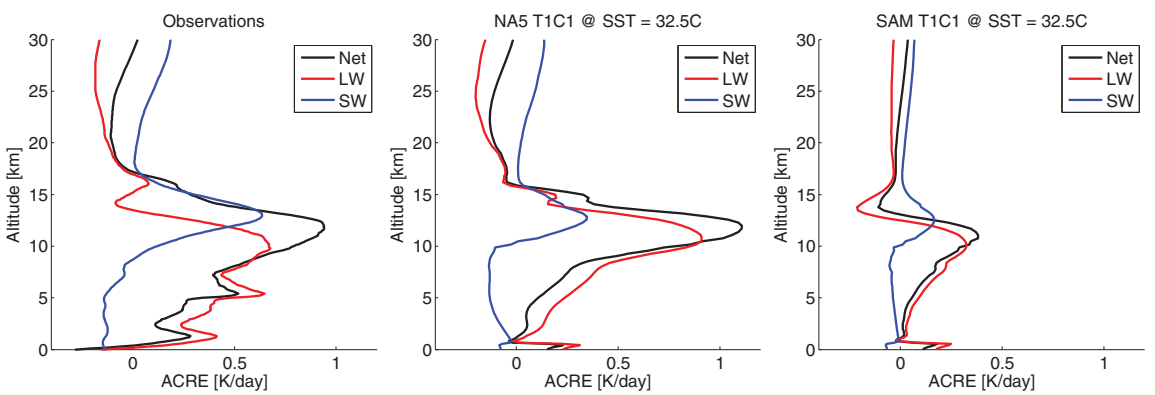


Figure 2. Atmospheric cloud radiative effect (ACRE) profiles for (left) observations, (middle) NA5 microphysics, and (right) SAM base microphysics. The longwave contribution is in red, the shortwave in blue, and the net in black.

3. Results

3.1. How Does Cloud Fraction Respond to ACRE?

The first question we wish to address is a direct follow-up to *Fu et al*. [1995]. Does ACRE increase the high cloud fraction? We will begin our analysis with the limited area domain simulations. Here we adopt the convention of high clouds as those clouds with a cloud top pressure (CTP) less than 440 hPa. Cloud fraction, or areal coverage as we will sometimes refer to it, is the fraction of the domain covered by cloud (defined as a column with cloud mass, combined liquid and ice, exceeding 0.02 kg/m^2). The cloud radiative heating decreases the high cloud fraction—from 39% to 27% for SST = 28.5°C and from 36% to 25% for SST = 32.5°C. The high cloud reduction can be seen as the difference between T1C1 and T0C0 for the two different SSTs in Figure 3 (top row). We expect that the reduction of cloud fraction by ACRE is the combination of the two effects of cloud radiative heating. The first is the radiative destabilization of the anvil and cirrus clouds, by heating at the bottom and cooling at the top (the direct effect). The second is the stabilizing effect on the temperature profile from the cloud heating (the indirect effect). To separately assess the direct and indirect cloud heating effects, we rely on our additional experiments.

The indirect cloud heating effect (the stabilizing of the troposphere to convection through heating of the upper troposphere by clouds) can be determined by differencing experiments T1C0 and T0C0 for a given domain size and sea surface temperature. In both T1C0 and T0C0 experiments, the clouds are radiatively inactive, but the mean radiative cloud heating still heats the environment and enhances the atmospheric stability in the T1C0 experiment. The indirect cloud heating effect can be isolated by differencing the T1C1 and T0C1 experiments. Thus, we are determining the influence of the indirect cloud heating effect by differencing "T1" experiments with their corresponding "T0" experiments.

For convenience, we will refer to the combination of the direct cloud heating effect and indirect cloud heating effect as the total cloud heating effect. The total cloud heating effect is determined by the difference in the T1C1 and T0C0 experiments for a given domain size and sea surface temperature.

Returning to Figure 3, we can see the role of the direct and indirect cloud heating effects on the cloud fraction profile. The direct cloud heating effect (T1C1–T1C0 or T0C1–T0C0) always leads to an increase in the cloud fraction. The increase in cloud fraction occurs primarily between 200 and 400 hPa, roughly the outflow layer for anvil clouds, as expected. The total high cloud fraction is significantly larger as a result of the direct cloud heating effect (significant at the 95% level). Significance is determined using a two sample *t*-test of the domain mean high cloud fraction sampled 200 times for each run (50 days of 6 hourly output). The increase in high cloud fraction is 11–13% for the high stability profile (T1) and 27–29% for the low stability profile (T0), both for the small-domain experiments (for the mock-Walker circulation experiments, the increase is 4–6%). Compared to the direct cloud heating effect, the indirect cloud heating effect has the opposite effect on the cloud fraction. The indirect cloud heating effect (T1C0–T0C0 or T1C1–T0C1) decreases the cloud fraction. The high cloud fraction decreases by 38–41% for the interactive cloud experiments (C1) and by 22–25% for the noninteractive cloud experiments (C0), both for the small-domain experiments (for the mock-Walker circulation experiments, the decrease is 3–6%).

From the above, the total cloud heating effect (T1C1–T0C0) is dominated by the indirect cloud heating effect, such that the high cloud fraction is reduced by 11–13% in the limited-domain simulations. In the mock-Walker circulation experiments, the total cloud heating effect on cloud fraction is small (1% or less) because the direct and indirect cloud heating effects balance one another. It should be noted that the vertically resolved cloud profiles are not the same between the T1C1 and T0C0 experiments, so while the areal coverage is insensitive to the total cloud heating effect, the cloud properties may not be. We will return to this point later.

We can ask whether the increase in cloud fraction owing to the direct cloud heating effect is in fact due to increased destabilization within the cloud layer. To investigate this feature, we first look at the turbulent kinetic energy (TKE) profiles for the same experiments presented in Figure 3. Figure 4 shows that the TKE in the upper troposphere shows a strong peak for the experiments with the direct cloud heating effect included (T1C1 and T0C1). Note that convection is stronger in both T0C1 and T0C0 experiments, as can be seen by the stronger TKE throughout the depth of the troposphere. Additionally, the presence of more clouds, as in the weaker stability cases, generates more TKE as well. Still, the difference in TKE between the cloud layer and the midtroposphere is largest when the direct cloud radiative heating effect is included.

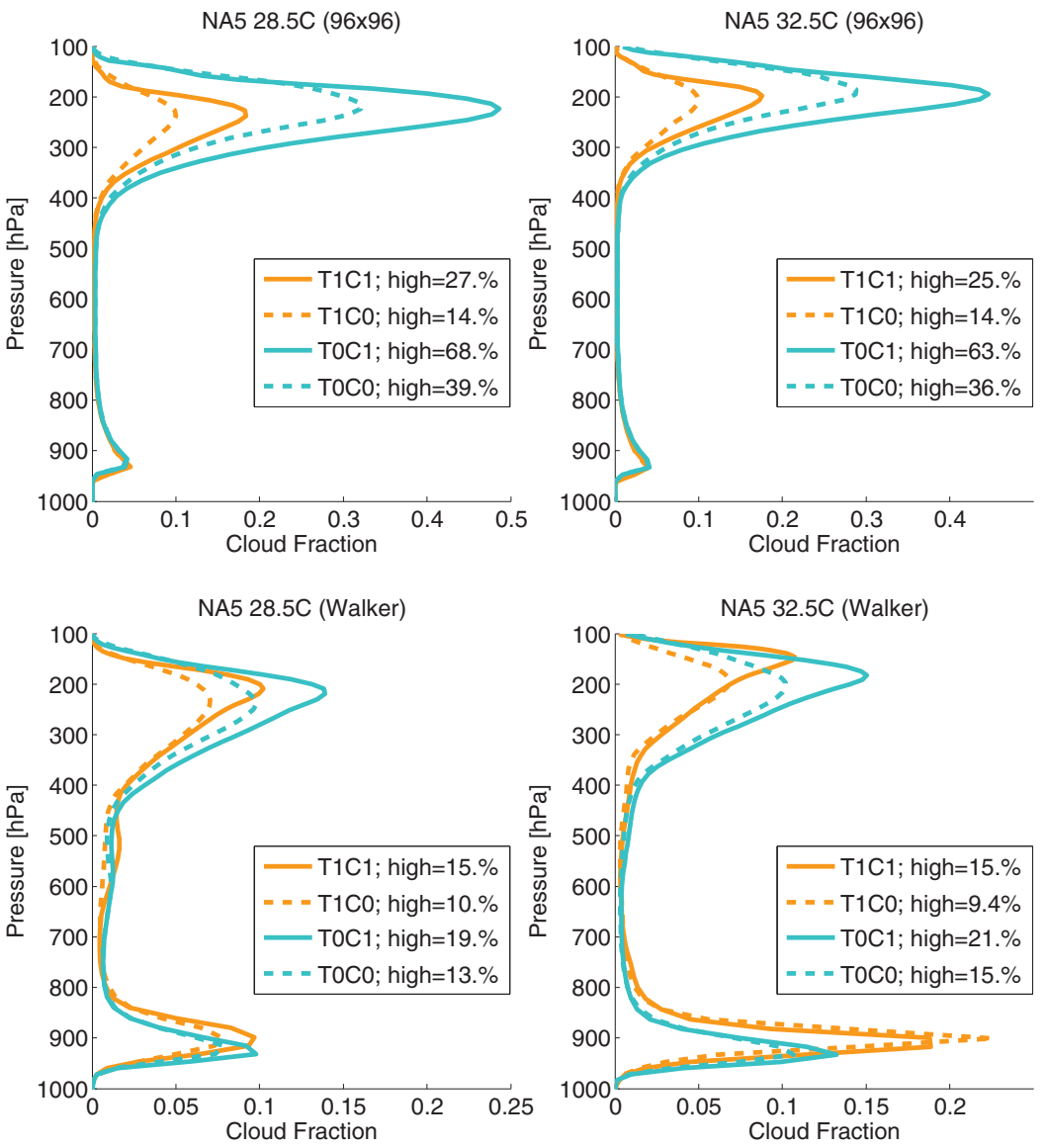


Figure 3. Cloud fraction profiles for (top) the limited-domain experiments and (bottom) the mock-Walker circulation experiments. (Left) the profiles for SST = 28.5°C and (right) the profiles for SST = 32.5°C. The domain mean high cloud fraction (CTP < 440 hPa) is given in the legend of each figure. Note that the cloud fraction axis changes between the small-domain (top row) and mock-Walker circulation (bottom row) experiments.

We are interested in asking how much of the turbulent motions are actually driven by the anvil and cirrus clouds. Is there any contribution from the deep convective cores? Convective cores are defined here as cloudy layers where the vertical velocity exceeds 1 m/s (either upward or downward) and the virtual potential temperature anomaly is greater than zero for updrafts (less than zero for downdrafts). The virtual potential temperature transport is calculated as $\overline{\theta_v w'}$, where the overbar denotes an average over regions that are cloudy, $\theta_v' > 0$, and $w' > 1$ m/s (or $\theta_v' < 0$ and $w' < 1$ m/s). This definition is somewhat different than the normal eddy flux of θ_v in that it selects only regions with $|w'| > 1$, but also selects regions that are within cloud. It also does not directly use θ_v' in the calculation, so the magnitude of the transport will vary from the normal eddy flux. We employ the vertical velocity criterion to select only the vigorous updrafts and downdrafts. We employ the virtual potential temperature threshold to identify updrafts that are correlated with warming, as opposed to mechanically driven. Thus, regions of nonconvective core cloud are those that are cloudy, but are not part of the strong updraft or downdraft regions of the convection. Figure 5 shows the transport of virtual potential temperature in regions of nonconvective core cloud. Virtual potential

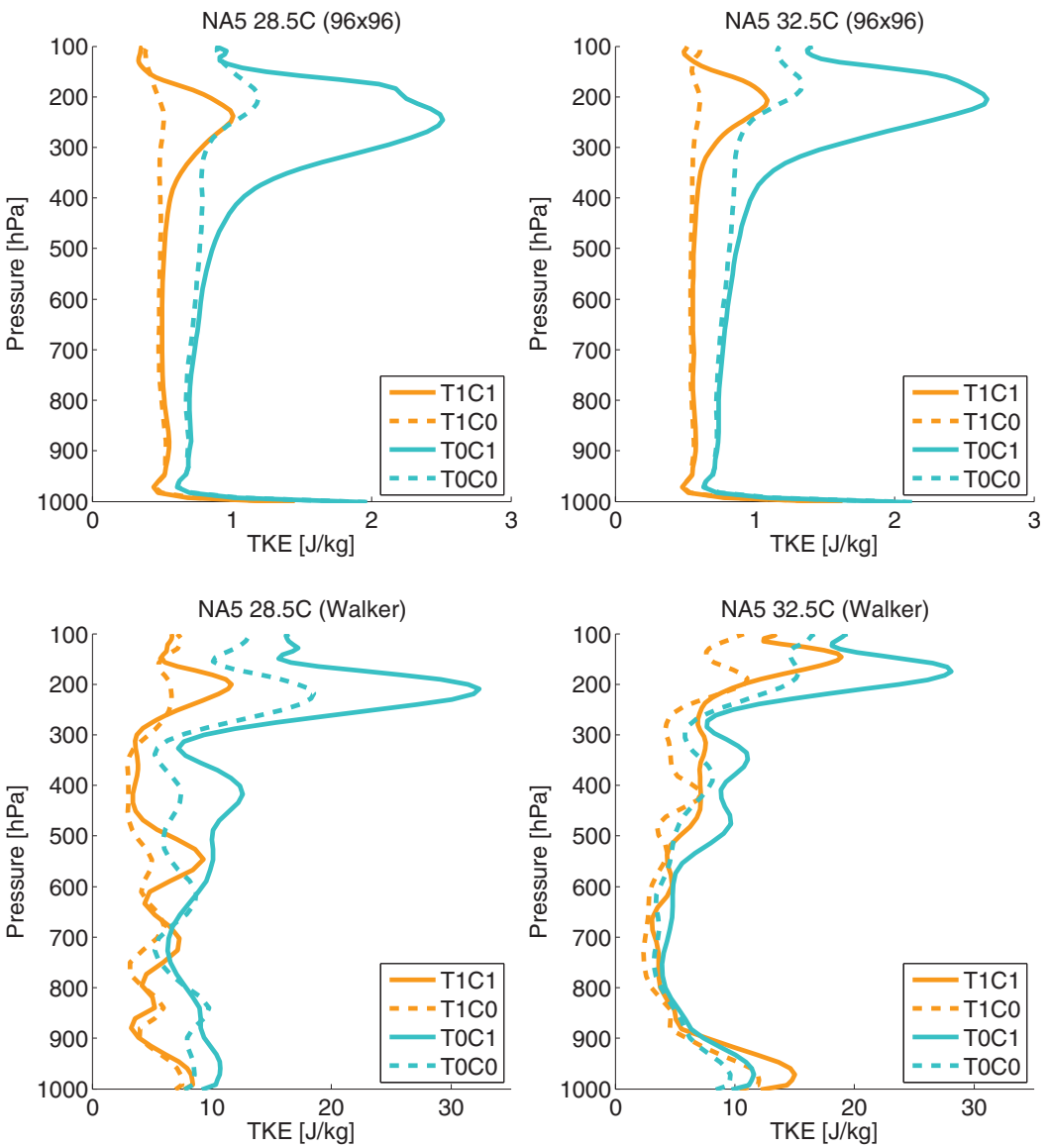


Figure 4. Same as Figure 3 only for turbulent kinetic energy (TKE) profiles.

temperature serves as a useful proxy for the buoyancy. Subtracting out the cores allows us to look at the effects of buoyancy transport in the anvil and cirrus clouds separated from the deep convection. Figure 5 shows that direct cloud heating effect more than doubles the θ_v transport within the clouds. The direct cloud heating effect does alter the θ_v profile some owing to the enhanced mixing generated, but those changes in θ_v owing to the direct cloud heating effect are less than 1 K (not shown). Therefore, the increase in transport must be driven by increases in vertical velocity within the clouds, driven by the direct cloud heating effect. Indeed, the mass flux profiles are similar to the energy transport profiles (not shown). Furthermore, the increase in the buoyancy transport occurs outside of the deep convective cores, and is instead associated with the anvil clouds and extensive cirrus within the model domain. The direct cloud heating effect is larger when the stability effect is not present. It can be seen in Figures 4 and 5 that in the more stable T1C1 experiment where convection is less frequent or weaker, less cloud is generated compared to the T0C1 experiment, and hence less cloud is present to interact with the radiation and generate turbulent kinetic energy or θ_v transport.

In the mock-Walker circulation experiments, we can see that the lower and middle troposphere show different responses to the direct and indirect cloud radiative heating effects compared to the limited-domain

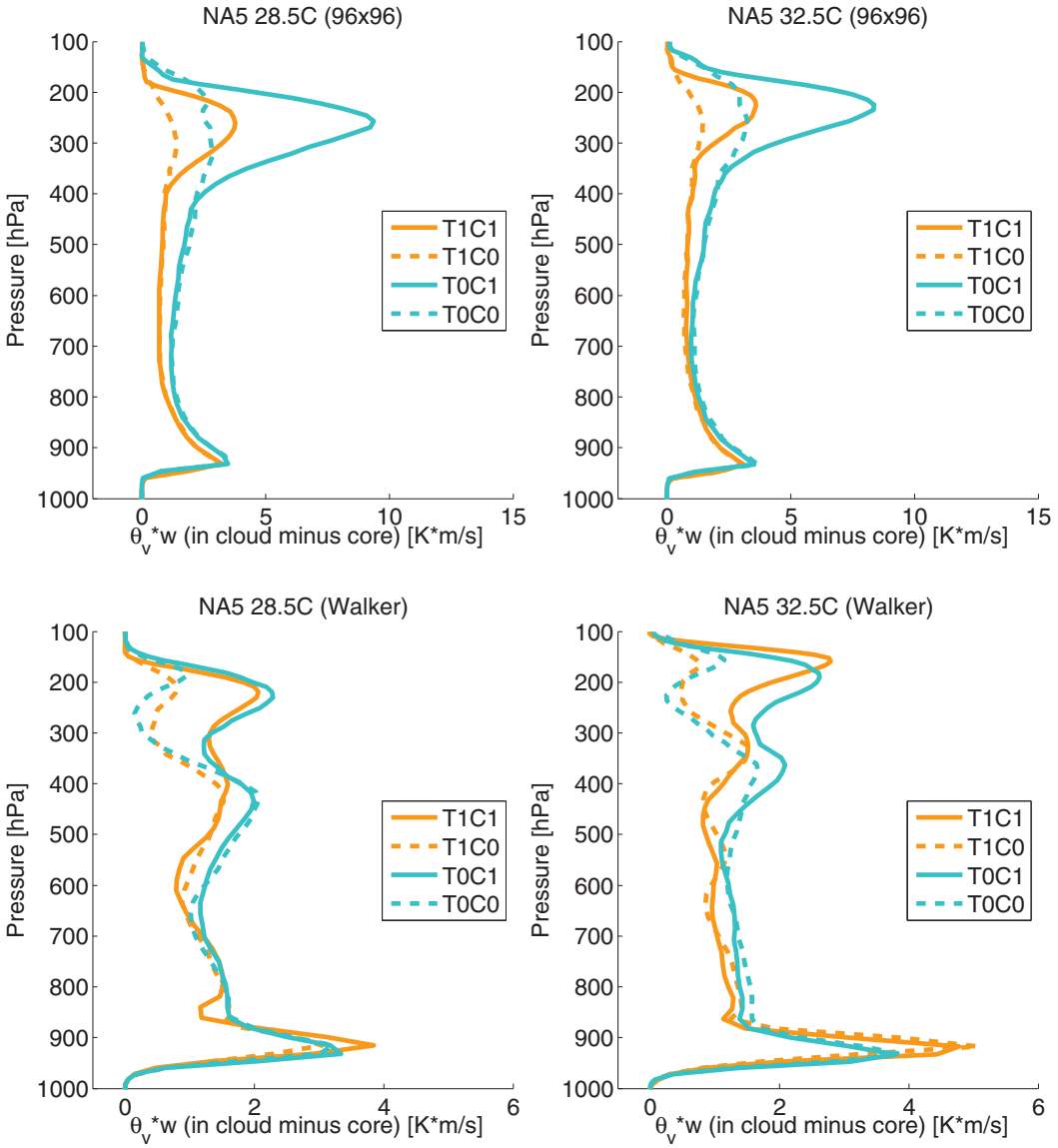


Figure 5. Same as Figure 3, but for θ_v transport in cloudy areas outside the convective cores. Positive values indicate upward energy transport.

experiments. The mock-Walker circulation experiments have a lot more low cloud, primarily over the cold pool regions of the domain, and radiation is important for their maintenance as well.

3.2. How Does the Top-of-Atmosphere Cloud Radiative Effect Respond to ACRE?

An increase in high cloud fraction can have a profound effect on the climate system. *Harrop and Hartmann* [2015] showed that for an increase in high cloud amount of 1%, top-of-atmosphere net CRE decreases by 0.26 W/m^2 (based on satellite retrievals over the West Pacific warm pool). In their study, changes in high cloud amount were determined as changes in the first empirical orthogonal function (EOF), which described an amplification of the mean cloud distribution in cloud optical depth/cloud top pressure space. Combining this value for CRE as a function of high cloud amount with the changes in high cloud fraction above, we calculate the CRE change one might expect to incur from these high cloud changes, all else being equal. The increase of ∼12% or ∼28% in high cloud fraction owing to the direct cloud heating effect would cause net CRE to decrease by 3.1 or 7.2 W/m^2. Likewise, the decrease of ∼39% or ∼24% in high cloud fraction owing to the indirect cloud heating effect would cause net CRE to increase by 10. or 6.1 W/m^2. These numbers are for the limited-domain experiments.

We do not expect, of course, that any change in CRE simply reflects a change in average high cloud fraction. Therefore, the next question we will address is how the top-of-atmosphere cloud radiative effect (CRE) responds to the interactions between clouds and radiation. Not only will we examine the same experiments as the previous subsection, but we also wish to identify which components of the clouds or environment produce the changes in CRE we see between different experiments. In other words, we seek to quantify how much of the change in CRE comes from changes in cloud fraction compared to how much comes from changes in the cloud radiative properties. To accomplish this, we first write the CRE equation following *Hartmann et al*. [2001] as:

$$\mathrm{CRE}=\sum_i A_i[S_0(\alpha_{\mathrm{clr}}-\alpha_i)+F_{\mathrm{clr}}-F_i], \tag{3}$$

where A_i is the fractional area coverage of cloud, S_0 is the top of atmosphere insolation, α_{clr} is the clear-sky albedo, α_i is the cloudy albedo, F_{clr} is the clear-sky OLR, and F_i is the cloudy OLR. The subscript "i" refers to the cloud type. We break the cloud into different types based on cloud top pressure and cloud optical depth using the standard histogram bins for the International Satellite Cloud Climatology Project (ISCCP) [*Schiffer and Rossow*, 1983; *Rossow and Schiffer*, 1991]. The equation above gives the CRE for each cloud type, and its sum gives the total CRE. To get the change in CRE between experiments, we can use the above equation to express the total difference in CRE as a sum of the differences in the various terms, plus a covariance term

$$\begin{aligned}\Delta\mathrm{CRE}=&\sum_i \Delta A_i[S_0(\alpha_{\mathrm{clr}}-\alpha_i)+F_{\mathrm{clr}}-F_i]+\sum_i A_i[S_0(\Delta\alpha_{\mathrm{clr}})]+\sum_i A_i[S_0(-\Delta\alpha_i)]+\\&\sum_i A_i[\Delta F_{\mathrm{clr}}]+\sum_i A_i[-\Delta F_i]+\sum_i \Delta A_i[S_0(\Delta\alpha_{\mathrm{clr}}-\Delta\alpha_i)+\Delta F_{\mathrm{clr}}-\Delta F_i]\end{aligned}. \tag{4}$$

Note that in equation (4), the change in clear-sky albedo is typically negligible, but we leave it in for completeness. Changes in clear-sky OLR are especially important when comparing across different sea surface temperatures. In order to separate the model clouds into the ISCCP histogram bins, we first calculate the cloud optical depth following *Lopez et al*. [2009] as:

$$\tau=\frac{3}{2}\sum_j\left(\frac{\mathrm{LWP}_j}{r_{\mathrm{liq}}}+\frac{\mathrm{IWP}_j}{r_{\mathrm{ice}}(T_j)}\right), \tag{5}$$

where τ is the cloud optical depth, LWP is the liquid water path, IWP is the ice water path, r_{liq} is the cloud liquid effective radius, r_{ice} is the cloud ice effective radius, T is the temperature, and the j index denotes an individual model layer. The SAM model assumes a fixed cloud liquid effective radius of 14 μm. The ice effective radius follows the CAM3 parameterization based on *Kristjánsson et al*. [2000] and is a function of temperature alone, with colder temperatures producing smaller effective radii, and hence, larger cloud optical depths for a constant IWP. These sizes are only used for the radiative transfer scheme. The microphysics is a single-moment scheme and does not have any requirements to be consistent with the radiative transfer calls in terms of effective radius. Future studies should investigate the robustness across different microphysics schemes (so long as they are still capable of producing realistic ACRE profiles).

The breakdown of CRE into its components allows us to describe the influence of the direct, indirect, and total cloud heating effect on the CRE as changes in cloud amount, cloud albedo, cloud OLR, clear-sky terms, and a covariance term. The cloud amount term is straightforward. A shift in the abundance of various cloud types will change the CRE based on the CRE values for the cloud types that become more frequent and those that become less frequent. The cloud albedo factor and cloud OLR factor may be interpreted as a change in the mean cloud albedo or cloud OLR in each histogram bin. For example, if the atmosphere warms at a given pressure level, the cloud OLR would change without a shift in the amount histogram. Likewise, changes in albedo can occur within a given histogram bin that are not accounted for by changes in the frequency of that bin. The primary benefit of breaking the CRE changes down into the ISCCP histogram is that it allows us to isolate the changes in CRE owing to the high clouds alone, simply by summing over the histogram bins where CTP $<$ 440 hPa. For simplicity, the following discussion will only focus on CRE changes owing to high clouds (CTP $<$ 440 hPa). It is worth noting that the CTP and cloud optical depth are calculated for each model column so that they are comparable to satellite retrievals. Table 1 shows the change in high cloud CRE breakdowns when comparing different experiments.

Table 1. Changes in Top-of-Atmosphere Cloud Radiative Effect (CRE) for High Clouds Only (CTP < 440 hPa)[a]

C1–C0	ΔA_i	$\Delta\alpha_{clr}$	$\Delta\alpha_i$	ΔF_{clr}	ΔF_i	Covariance	Total
T1 28	1.81	−0.00	0.78	0.02	−0.88	−0.19	1.55
T0 28	5.35	0.01	1.51	0.34	−1.49	−0.07	5.65
T1 32	0.99	0.00	0.52	0.00	−0.39	0.02	1.14
T0 32	4.89	0.00	1.17	0.18	−1.02	−0.15	5.07
T1 28w	0.41	−0.00	0.39	0.28	−0.38	0.09	0.78
T0 28w	1.06	−0.00	−0.07	0.09	0.18	0.06	1.32
T1 32w	0.09	0.00	0.30	0.64	−0.27	0.45	1.21
T0 32w	0.29	0.00	0.13	0.59	−0.00	0.25	1.26
T1–T0							
C1 28	1.59	−0.08	4.67	−0.45	−11.92	4.75	−1.44
C0 28	4.06	−0.04	1.97	0.02	−5.46	2.11	2.66
C1 32	0.24	−0.07	2.95	−0.31	−8.68	3.53	−2.33
C0 32	3.12	−0.04	1.38	−0.01	−4.69	1.84	1.60
C1 28w	0.01	−0.02	0.73	−0.56	−1.25	0.23	−0.87
C0 28w	0.44	−0.01	−0.05	−0.66	−0.27	0.22	−0.33
C1 32w	−1.33	−0.00	2.30	2.22	−4.13	−0.04	−0.98
C0 32w	−0.93	−0.01	1.28	1.19	−2.46	−0.01	−0.93
32–28							
T1 C1	0.23	−0.11	1.07	1.41	−2.82	0.16	−0.05
T1 C0	0.75	−0.06	0.76	0.76	−1.90	0.04	0.36
T0 C1	0.89	−0.27	4.23	3.47	−8.30	0.82	0.85
T0 C0	1.21	−0.15	3.18	2.13	−5.29	0.34	1.42
T1 C1w	−0.54	−0.05	2.61	2.96	−5.16	0.64	0.46
T1 C0w	−0.18	−0.04	2.08	1.68	−3.63	0.11	0.02
T0 C1w	0.99	−0.08	1.99	1.22	−3.73	0.18	0.57
T0 C0w	1.42	−0.06	1.24	0.44	−2.35	−0.06	0.63
T1C1–T0C0							
28	7.15	−0.04	3.91	0.08	−7.83	0.93	4.21
32	5.32	−0.04	2.35	0.00	−5.38	0.48	2.75
28w	1.14	−0.02	0.45	−0.31	−0.71	−0.10	0.45
32w	−0.79	0.00	1.77	2.22	−2.90	−0.02	0.28

[a]All values are expressed in W/m^2. A "w" indicates a mock-Walker simulation. The factors use the same notation as equation (4).

First, Table 1 shows that the direct cloud heating effect increases the CRE from the high clouds, making it less negative. The increase in CRE is greater when stability is weaker and high clouds are more abundant than for the cases where the stability is higher and high clouds are less abundant. For the limited-domain experiments, the cloud amount, cloud albedo, and cloud OLR are the dominant factors in determining the total CRE increase. The cloud albedo and cloud OLR changes are largely offsetting, however, such that the total CRE increase is quite similar to that predicted solely by the change in cloud amount. Figure 6 shows the breakdown of the CRE change from the direct cloud heating effect. We can see that some cloud types contribute to the increase in CRE, while other cloud types decrease the CRE. Most of the increase in CRE comes from the cirrus (CTP $<$ 440 hPa and $\tau < 3.6$). Deep convection (CTP $<$ 440 hPa and $\tau > 23$) and cirrostratus (CTP $<$ 440 hPa and $3.6 < \tau < 23$) have counterbalancing effects on CRE. The changes in the highest clouds (CTP $<$ 180 hPa), increase CRE, while slightly lower clouds (180 hPa $<$ CTP $<$ 440 hPa) decrease CRE. Figure 7 shows the change in cloud amount for each cloud type. As for CRE, most of the increase occurs for the cirrus clouds. The anvil clouds (cirrostratus) also increase, giving rise to the counterbalancing negative CREs seen in these bins. There is very little change in the cloud amount in the highest cloud top pressure bins.

Figure 6 looks similar to an amplification of the basic CRE ISCCP pattern (not shown) with the notable exception of clouds with CTP $<$ 180 hPa and $\tau > 3.6$. For clouds whose CTP $>$ 180 hPa, there is an increase in CRE for cloud types that have a positive CRE and a decrease for those cloud types that have a negative CRE. In other words, the CRE for these clouds is amplified. *Webster and Stephens* [1980] suggested that the direct effect would be more important for weakly precipitating clouds, and *Ackerman et al.* [1988] also suggested that thin anvils would be more susceptible to the effects of radiative destabilization than thicker anvils. Both of these studies suggest that the thicker clouds are less susceptible to the direct effect than the thinner ones. Figure 6 is in agreement since the largest change in CRE occurs for the thinner clouds. Figure 8 shows the ISCCP histogram for each of the limited-domain experiments. Compared to observations [see *Harrop and Hartmann*, 2015, Figure 7], cirrus are favored over anvil clouds in our model. Our modeled

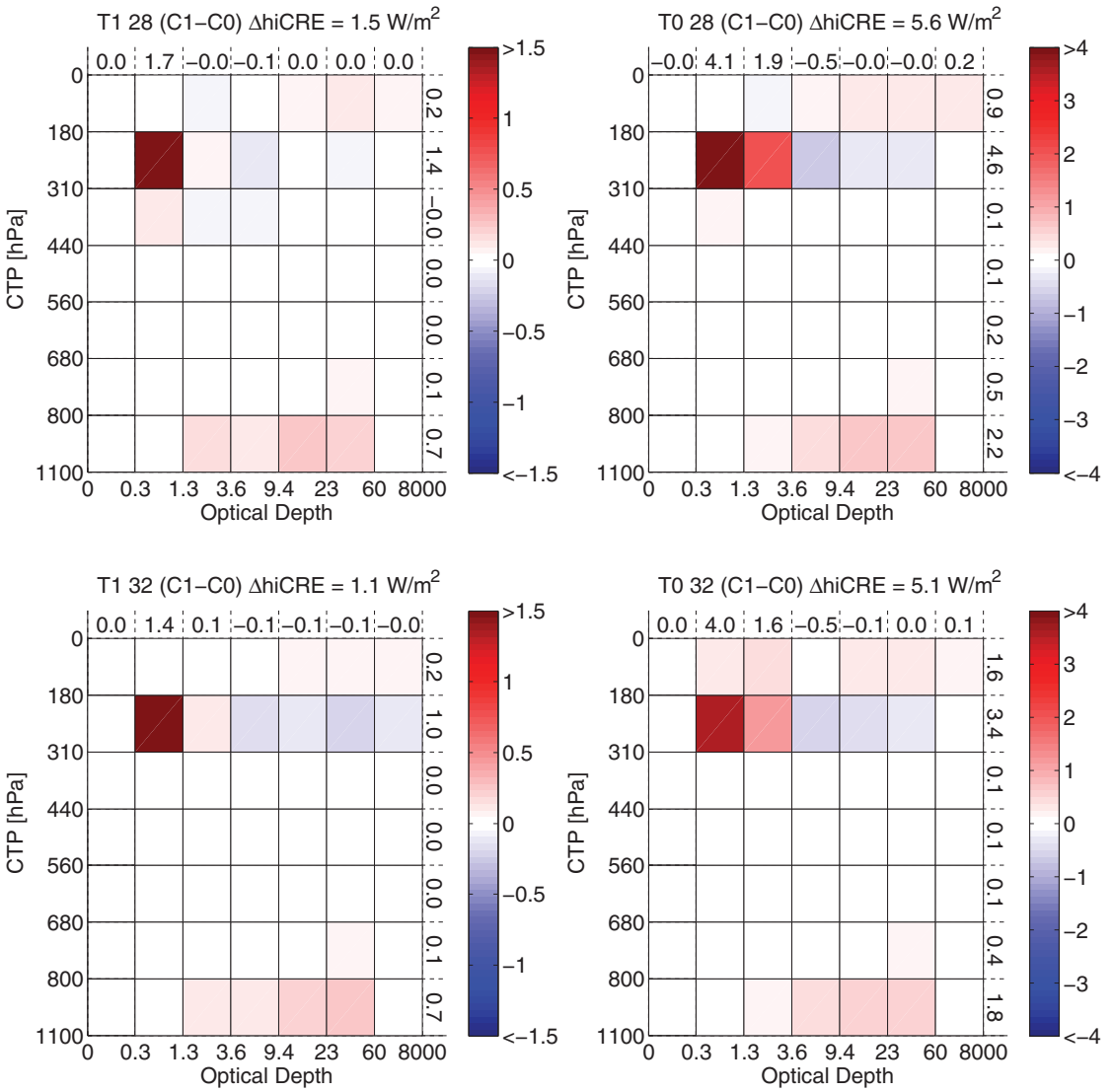


Figure 6. Change in CRE for each bin of the ISCCP histogram owing to the direct cloud heating effect. The total high cloud ΔCRE is given in the title of each plot. The top row is for SST = 28.5°C and the bottom row is for SST = 32.5°C. The left column is for the strong stability experiments (T1) and the right column is for the weak stability experiments (T0). Note that the color scale changes between the left column and the right column. The numbers along the top are the change in high cloud CRE for each optical depth bin summed over all cloud top pressures. The numbers along the right side are the change in all-cloud CRE for each CTP bin summed over all optical depths.

clouds also tend to fall in the 180–310 hPa cloud top pressure bin. Without a Brewer-Dobson circulation, however, our tropopause is likely to be too low in the model.

We can perform the same breakdown of which cloud types contribute to the change in CRE when driven by the indirect cloud heating effect as well. Figure 9 shows the same plots as Figure 6, but for the stability differences owing to the indirect cloud heating effect. The increase in stability tends to reduce cloud amounts for all high clouds (Figure 10) and this is reflected in the change in CRE ISCCP histograms in Figure 9. The high, thin clouds that have a positive CRE are reduced, causing a decrease in the total CRE, while the high, thick clouds that have a negative CRE are also reduced, causing an increase in the total CRE. When the direct cloud heating effect is included, more high, thin clouds are lost when stability increases, such that the change in CRE is negative. When the direct cloud heating effect is removed, the opposite occurs. Fewer high, thin clouds are present, so the reduction of clouds is weighted toward the thick clouds and thus, the change in CRE is positive. The covariance terms for the indirect cloud heating effect are the same order of magnitude as the other terms. Therefore, the CRE changes cannot be as simply interpreted for the indirect cloud heating effect as they were for the direct cloud heating effect.

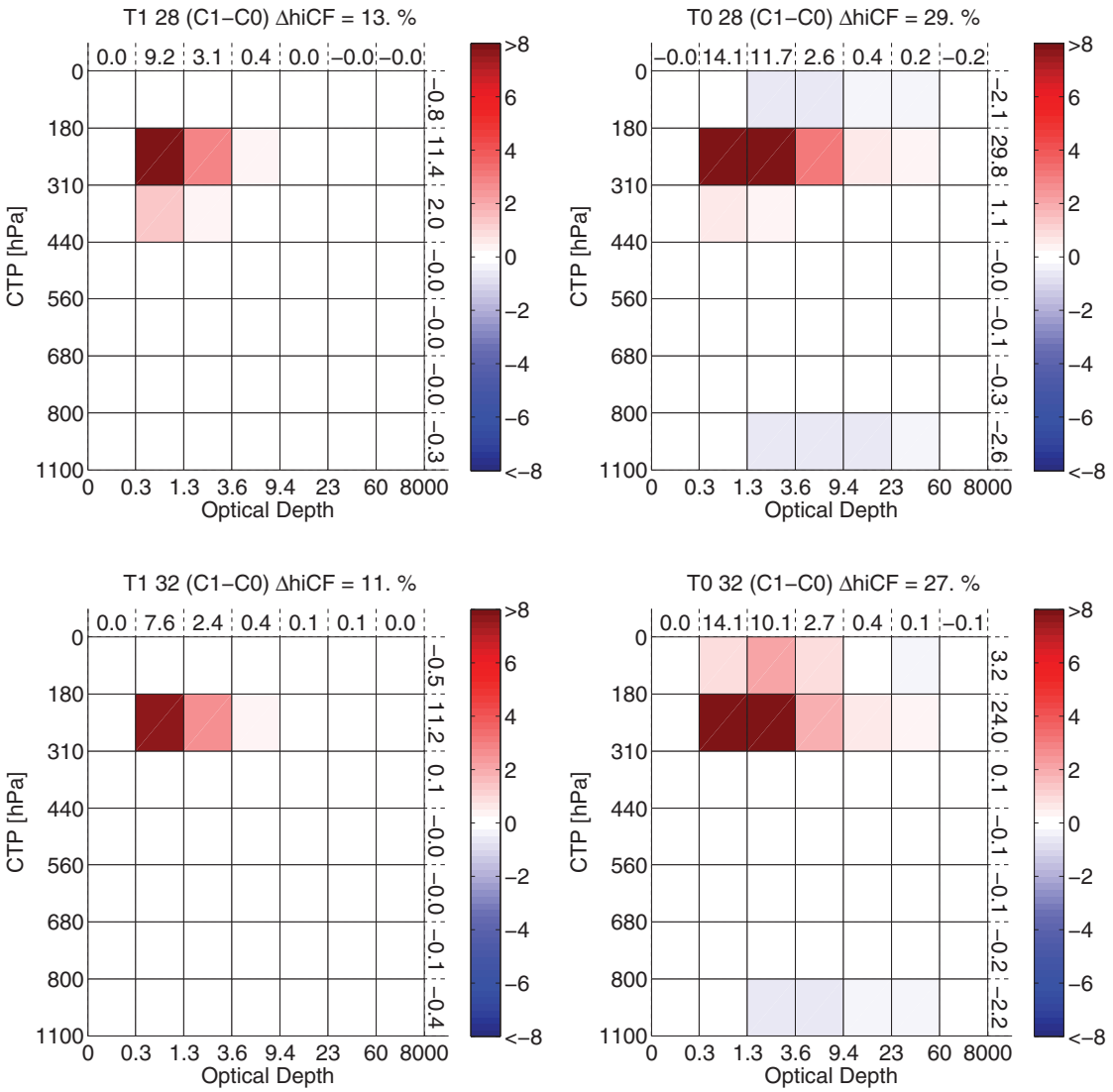


Figure 7. Change in cloud fraction for each bin of the ISCCP histogram owing to the direct cloud heating effect. The total high cloud fraction change is given in the title of each plot. The top row is for SST = 28.5°C and the bottom row is for SST = 32.5°C. The left column is for the strong stability experiments (T1) and the right column is for the weak stability experiments (T0). The numbers along the top are the change in high cloud fraction for each optical depth bin summed over all cloud top pressures. The numbers along the right side are the change in total cloud fraction for each CTP bin summed over all optical depths.

The changes in CRE for increasing sea surface temperature are dominated by the clouds rising. The clouds rise in such a fashion that the cloud amount does not change much (not shown). If we refer back to Table 1, we see that the cloud amount changes indeed account for very little of the total CRE change for sea surface temperature. Instead, the CRE is dominated by changes in cloud albedo and the clear- and cloudy-sky OLR. The albedo and clear-sky OLR increase the CRE, while the cloudy-sky OLR decreases CRE. The three terms largely cancel one another, such that the total change in CRE with warming is small. We expect the clear-sky OLR to increase CRE since clear-sky OLR will increase in a warmer atmosphere. The albedo response implies the clouds are thinning in a warmer atmosphere, while the cloudy-OLR response implies the clouds are warming some. It has been shown that high clouds do not rise exactly isothermally with increasing SSTs in this CRM owing to the fixed ozone profile impacting stability [see *Harrop and Hartmann*, 2012]. The ozone stability limits the rise of the clouds, causing them to occur at slightly warmer temperatures than what is predicted by the Fixed Anvil Temperature (FAT) hypothesis [e.g., *Hartmann and Larson*, 2002; *Kuang and Hartmann*, 2007; *Zelinka and Hartmann*, 2010; *Harrop and Hartmann*, 2012]. Because the change in SST is 4 K for each of the SST differences in Table 1, the feedback would be small for all of the ΔSST experiments (−0.01, +0.09, +0.2, +0.4 W/m^2).

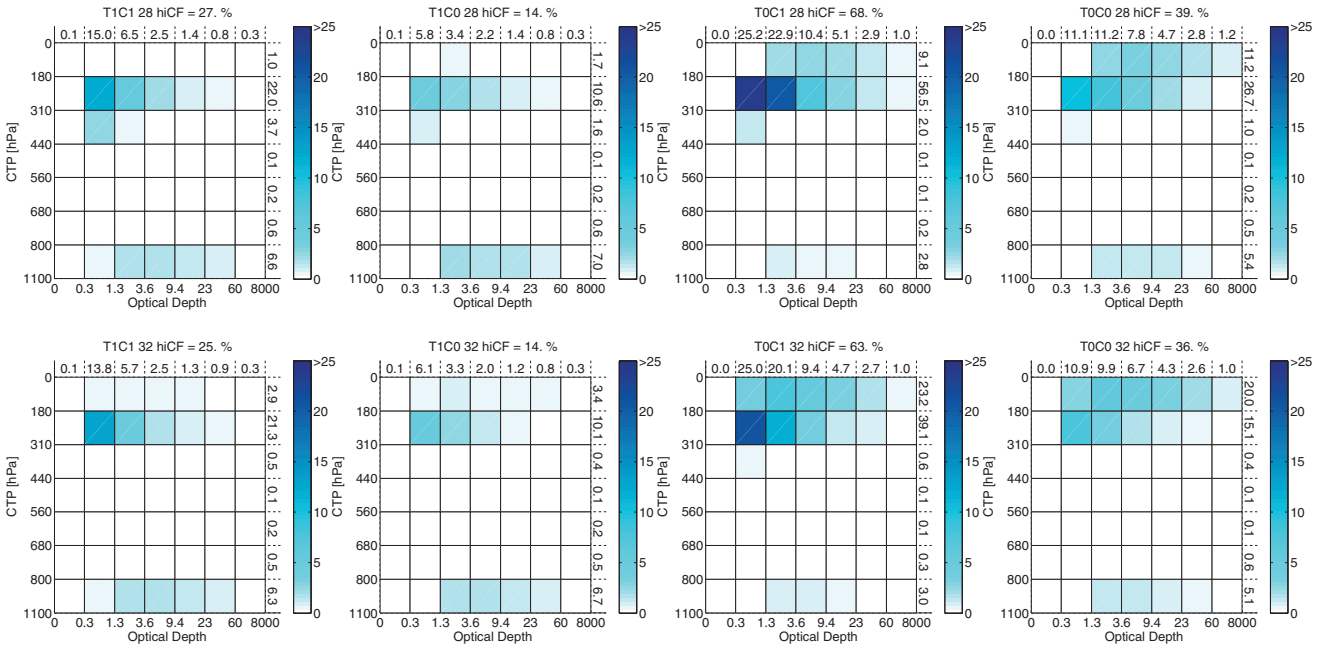


Figure 8. Cloud fraction ISCCP histograms for the limited-domain experiments. The value of each histogram is A_i from equation (3). The top row is for SST = 28.5°C and the bottom row is for SST = 32.5°C. Like Figure 7, the numbers along the top are the change in high cloud for each optical depth bin summed over all cloud top pressures. The numbers along the right side are the change in all-cloud fraction for each CTP bin summed over all optical depths.

We have focused on the high cloud changes in our discussion above. As noted in section 2, the model grid spacing is insufficient to accurately simulate low clouds. As such, we do not have confidence in the low cloud changes, or their impact on the top-of-atmosphere CRE. Also, there are very few low clouds in the limited-domain experiments, which is a result of the microphysics modifications we use. Despite this lack of confidence and underestimate in low cloud amount, our experiments show a consistent reduction in low cloud owing to the direct cloud heating effect and an increase in low cloud owing to the indirect cloud heating effect. Because all low clouds have a negative CRE over tropical oceans, the reduction (increase) in low cloud decreases (increases) the TOA CRE. The amounts of these changes can be found on the right side of the bottom two rows in Figures 6–9, and 10.

Finally, the total cloud heating effect shows an increase in CRE. Again, we see that the clouds thin and warm such that cloud albedo changes invoke an increase in CRE while cloud OLR changes invoke a decrease in CRE. The decrease in total cloud amount leads to an increase in CRE.

In this section, we have shown the effect of ACRE on the cloud radiative effect from high clouds. The direct effect increases high cloud fraction, while at the same time shifting the pdf of cloud optical depths toward thinner clouds and warming the cloud tops. The combination of the change in cloud optical depth and cloud top temperature increases the CRE (making it less negative). The indirect effect, on the other hand, decreases high cloud fraction, while simultaneously shifting the cloud optical depth pdf toward thinner clouds and warming the cloud top temperatures, like the direct effect. While the indirect effect tends to dominate the response of the high cloud fraction, the direct effect has a larger impact on CRE.

Most of our discussion has focused on the limited area domain simulations since they are the more straightforward. It should be noted that, again, like the high cloud fraction changes, many of the changes in CRE owing to the direct, indirect, and total cloud heating effects show similar behavior in the mock-Walker circulation experiments as those in the limited-domain experiments. We will elaborate on the differences in section 3.3.

3.3. Does a Large-Scale Circulation Mitigate the Stability Effect of the Cloud Radiative Heating?

We have focused much of our previous analysis on the limited area domain experiments because they are simpler by construction and easier to understand. The inclusion of a large-scale circulation pattern

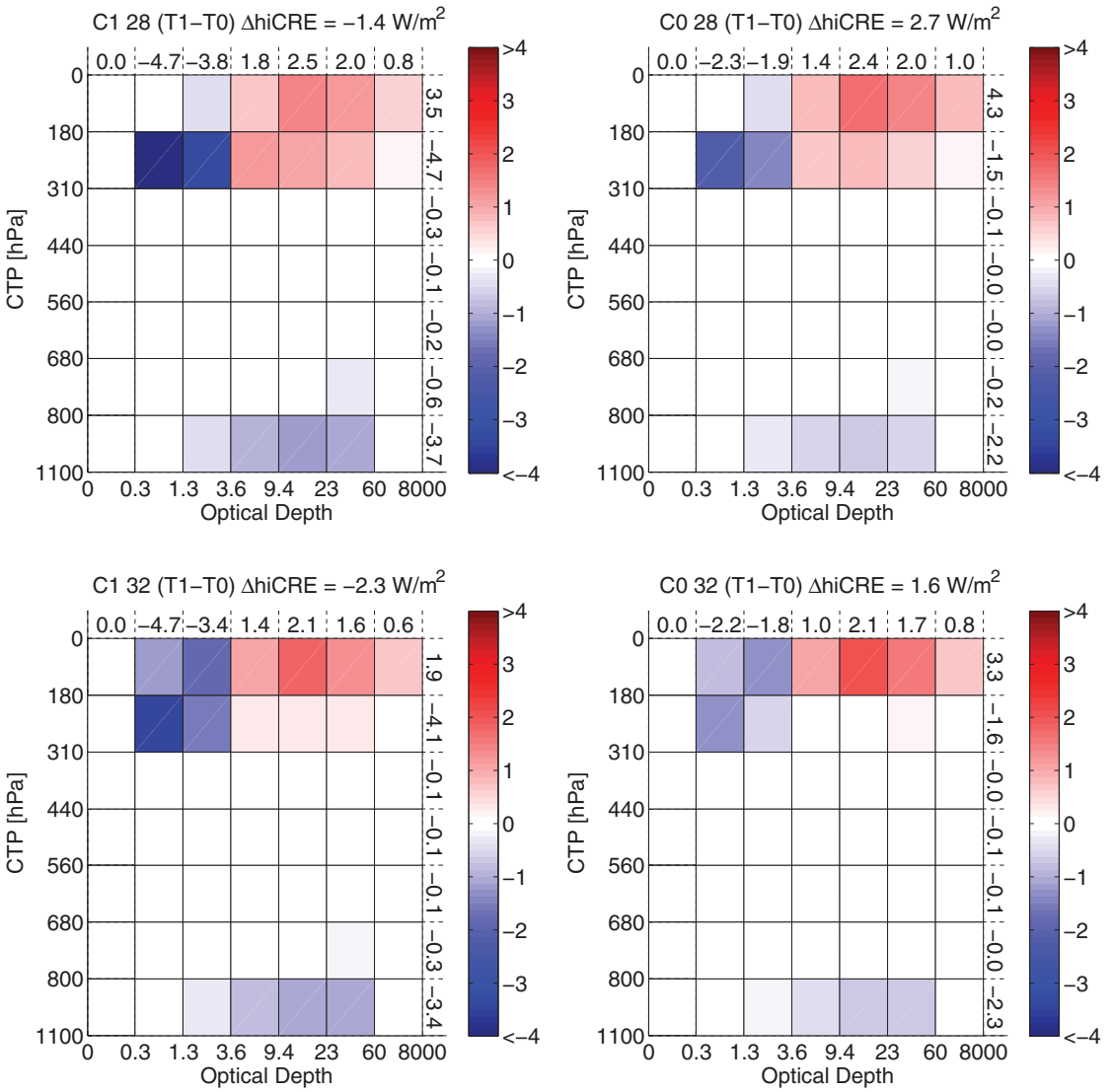


Figure 9. Same as Figure 6, but for differences in the indirect cloud heating effect (T1–T0).

complicates some of the analysis because there is an additional feedback within the system associated with spatial gradients in ACRE and their effect on circulation strength. Despite the added complexity, many of the responses of the clouds and the top-of-atmosphere cloud radiative effect (CRE) are the same as those seen in the limited area domain experiments (see Table 1). The biggest difference is that of the indirect cloud heating effect.

In a system with both a warm pool and cold pool, the large-scale circulation is capable of transporting some of the energy of ACRE heating from the warm pool to the cold pool. The cold pool can be thought of as a more effective sink of energy, or a "radiator fin" as described by *Pierrehumbert* [1995]. Thus, the mock-Walker circulation atmosphere does not collect the heat from the clouds and grow quite as stable as it does in the limited area domain experiments. The changes in cloud fraction owing to either the direct or indirect cloud heating effect are muted compared to the limited area domains, as noted earlier, and the overall cloud fraction in the domain is less (see Table 2).

The changes in CRE in the mock-Walker circulation are less straightforward than the changes in cloud fraction. While the total changes in direct cloud heating effect are more or less the same as the limited area domain experiments, in the mock-Walker circulation experiments, the clear-sky OLR also becomes an important factor (see Table 1). Because we have added in the domain mean ACRE uniformly instead of preserving

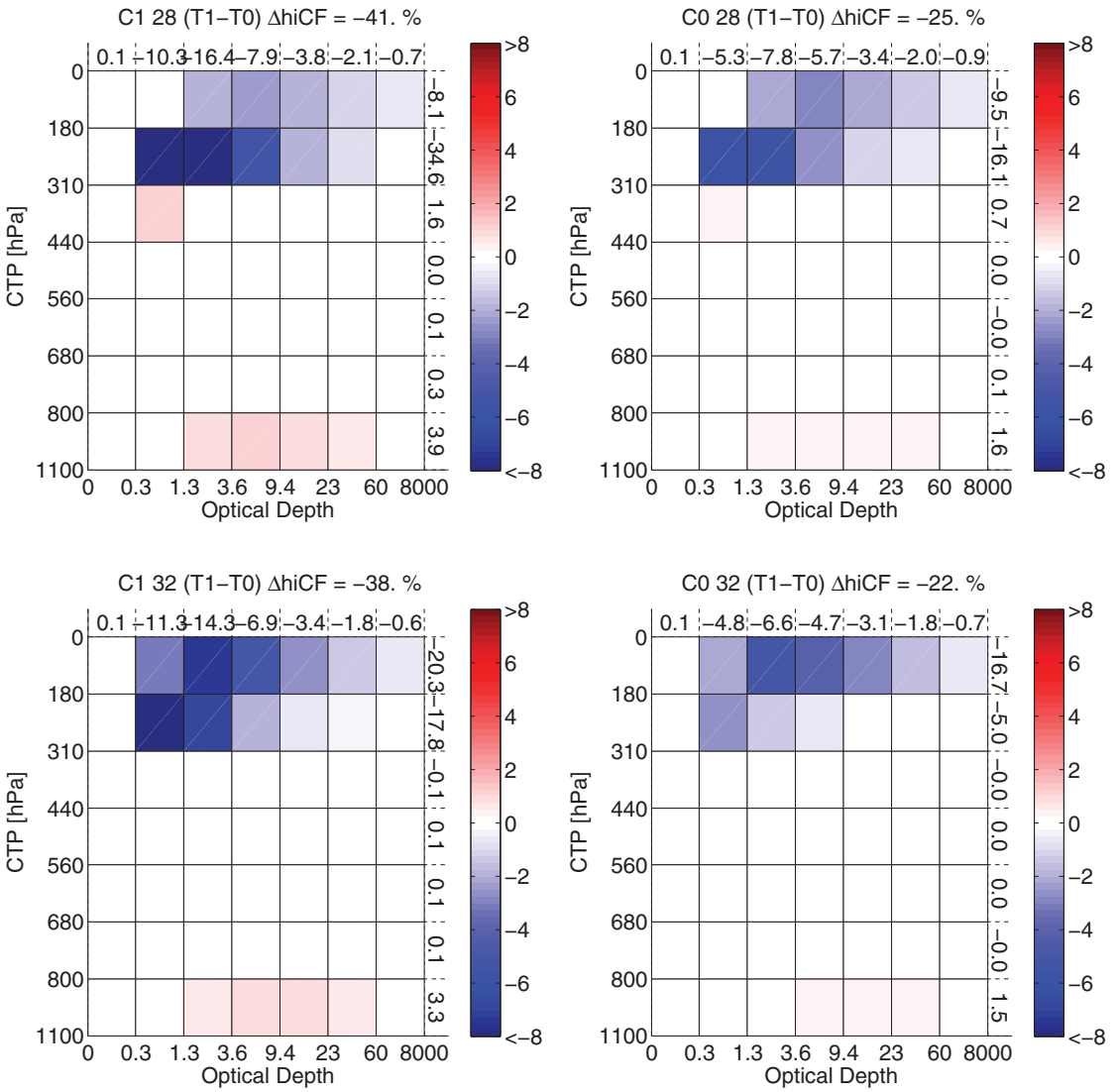


Figure 10. Same as Figure 7, but for differences in the indirect cloud heating effect (T1–T0).

the time-averaged spatial structure, changes in the circulation occur, and these changes alter the temperature and humidity profiles, and hence the clear-sky OLR.

The change in cloud fraction owing to the total cloud heating effect is small, and therefore the increase in CRE owing to the cloud fraction factor is likewise small. The albedo, clear- and cloudy-sky OLR changes are nonnegligible, but are largely offsetting, such that the net CRE change in response to the total cloud heating effect is small. Interestingly, the changes in CRE owing to sea surface temperature increase in the mock-Walker circulation experiments are not distinct (both in total and component breakdown) from the limited-domain experiments, suggesting that these effects may be robust to the presence of the circulation. However, the net change in CRE with SST is small compared to largely offsetting changes in OLR (both cloudy and clear) and cloudy albedo, allowing the small terms like cloud amount changes to potentially be important. Since the cloud amount changes are not consistent between the small-domain and mock-Walker experiments, more explicit testing in a global-scale circulation is needed to investigate the CRE response to SST further.

As we have already noted above, the decomposition into the direct and indirect effects is not exact in the mock-Walker experiments. These experiments do illustrate the point that the balance between stabilizing by warming (the indirect effect), and destabilizing by lifting or mixing through the large-scale circulation is

Table 2. Averages for Precipitation, ACRE, High Cloud CRE, High Cloud Fraction, and the Ratio of Driest to Wettest Water Vapor Path (WVP) Quartiles (Standard Deviation in Parentheses)[a]

Name	Precipitation (mm/d)	ACRE (W/m^2)	High CRE (W/m^2)	High CF (%)	D/W WVP
T1C1 28	2.5 (0.35)	27 (5.8)	−0.58 (2.0)	27 (6.8)	0.97
T1C0 28	2.5 (0.38)	16 (4.5)	−2.1 (2.1)	14 (4.7)	0.97
T0C1 28	3.1 (0.59)	78 (11)	0.86 (5.6)	68 (11)	0.95
T0C0 28	3.1 (0.48)	55 (7.5)	−4.8 (4.2)	39 (7.3)	0.96
T1C1 32	3.0 (0.46)	28 (6.4)	−0.63 (2.1)	25 (7.4)	0.97
T1C0 32	3.0 (0.47)	18 (4.8)	−1.8 (2.0)	14 (4.6)	0.97
T0C1 32	3.7 (0.69)	76 (12)	1.7 (5.7)	63 (12)	0.96
T0C0 32	3.7 (0.69)	52 (10)	−3.4 (4.2)	36 (9.3)	0.96
T1C1 28w	3.4 (1.1)	8.9 (3.2)	−0.87 (1.1)	15 (3.7)	0.41
T1C0 28w	3.4 (1.2)	6.9 (3.6)	−1.7 (1.2)	10 (3.4)	0.39
T0C1 28w	3.8 (2.2)	15 (5.2)	−0.0 (2.0)	19 (4.8)	0.43
T0C0 28w	3.7 (2.0)	11 (5.1)	−1.3 (2.0)	13 (4.4)	0.44
T1C1 32w	4.6 (2.9)	7.3 (4.3)	−0.41 (1.6)	15 (4.2)	0.32
T1C0 32w	4.4 (2.2)	2.6 (3.1)	−1.6 (1.2)	9.4 (3.0)	0.33
T0C1 32w	4.3 (2.4)	17 (4.2)	0.58 (1.9)	21 (4.1)	0.43
T0C0 32w	4.1 (2.2)	13 (4.9)	−0.69 (2.0)	15 (4.4)	0.48

[a]A "w" indicates a mock-Walker simulation.

a key issue. The relative importance of these two things depends on the scale of the circulation. Regardless, these experiments still point to the conclusion that one must simulate the indirect and direct effects accurately to get a realistic answer (as was found for the small-domain experiments). Future research should focus on the sensitivity of the relative contributions of the direct and indirect effects to organization of convection or the strength of the circulation.

3.4. What are the Implications for Cloud Feedbacks?

From the above, we have seen that the direct cloud radiative heating effect increases cloud fraction, while the indirect cloud heating effect decreases cloud fraction. The latter of these two is effectively a negative feedback on high cloud fraction. For a decrease in cloud cover, there will be an additional decrease in stability owing to the indirect cloud heating effect. The decrease in stability will favor more convection, and more clouds, thus reducing the initial perturbation. In a warmer climate, the tropical circulation is expected to slow [*Vecchi and Soden*, 2007]. A decrease in cloud amount would be expected to accompany the decrease in mass flux, with a negative feedback on the cloud amount from the indirect cloud heating effect response.

As the climate warms, clouds rise by the Fixed Anvil Temperature (FAT) hypothesis [e.g., *Hartmann and Larson*, 2002; *Kuang and Hartmann*, 2007; *Zelinka and Hartmann*, 2010; *Harrop and Hartmann*, 2012]. All else equal, a rise in the clouds would increase ACRE since the warmer lower troposphere emits more longwave radiation, while the fixed cloud top temperature would mean the clouds emit the same amount of longwave radiation as they did in the cooler climate. Therefore, the heating at anvil cloud base would be expected to increase, while the cooling at the cloud top would remain fixed. This would enhance the destabilization within the cloud layer, as well as increase ACRE within the column, and thus, increase both the direct and indirect cloud heating effects. In our experiments, ACRE increases by about 1–2% (W/m^2/K) when normalized by cloud fraction in the limited-domain simulations. The mock-Walker circulation experiments show no consistent response of ACRE to SST.

The total change in ACRE is likely to be small owing to the opposing ways in which the rising of clouds via the FAT mechanism increases ACRE and the decrease in cloud abundance through the circulation slowdown decreases ACRE. Comparing integrated domain mean ACRE across the warming experiments in our simulations, we see that ACRE does indeed show little change with sea surface temperature increase. As a result, the indirect cloud heating effect is likely to remain nearly the same as the climate warms. The direct cloud heating effect, the destabilization of the cloud layer, however, is still likely to increase, since it will be impacted more by the clouds rising. Climate models generally predict a reduction in cloud amount over the tropical warm pool [*Zelinka et al*., 2012], which is in agreement with a reduction in mass flux. It is unlikely that the physics of the anvil spreading by radiative destabilization is captured by these climate models, and as a result, the models may be overpredicting the reduction in cloud amount due to warming in the tropical

warm pool. Since the direct cloud heating effect leads to more high, thin clouds, not having the direct cloud heating effect in GCMs may also lead to an underprediction in climate sensitivity.

An increase in ACRE with warming is also likely to thin the clouds and warm the clouds. While these effects tend to cancel one another at the top of the atmosphere, it does so by reducing both the SWCRE and LWCRE. The SWCRE and LWCRE offsetting one another can be thought of as repartitioning energy between the ocean and the atmosphere [*Zhang and Rossow*, 1997; *Tian et al*., 2001]. Thus, the thinning and warming of the clouds owing to an increase in ACRE would effectively be partitioning more energy into the ocean at the expense of the atmosphere.

The FAT response is a feedback, but there is great interest in the so-called fast adjustments that are not dependent on surface temperature change. An instantaneous doubling of CO_2, for example, can elicit cloud changes in much the same way as ACRE. Making the atmosphere more opaque would limit the surface and lower atmospheric upwelling longwave radiation and thus reduce the direct cloud heating effect. As we have seen above, a reduction in the direct cloud heating effect will reduce high cloud fraction, it will shift the cloud optical depth toward thicker values, cool the clouds, and decrease the CRE. The fast responses of clouds are typically expected to increase CRE by reducing cloud fraction, so the ACRE response may negate some of that change.

4. Conclusions

We show that the atmospheric cloud radiative effect (ACRE) affects the high cloud fraction in two ways. First, the turbulence generated by longwave warming at cloud bottom and cooling at cloud top enhances the areal extent of the cloud, consistent with earlier findings [e.g., *Fu et al*., 1995]. Second, the net ACRE is a heating term that stabilizes the atmosphere and reduces cloud cover. In a limited area domain, the stability (or indirect) effect is the dominant control. In a mock-Walker circulation, the two effects largely cancel one another, owing to the ability of the large-scale circulation to transport heat from the warm pool to the cold pool, where it is removed by emission to space.

The cloud fraction is not the only aspect of the clouds that ACRE changes. In consequence of the direct cloud radiative heating effect, the average cloud optical depth decreases and cloud top temperature increases, and these are reflected in an increase in the top-of-atmosphere cloud radiative effect (CRE; making it less negative). By breaking down the change in CRE into its component cloud fraction, clear-sky albedo, clear-sky OLR, cloudy-sky albedo, cloudy-sky OLR, cloud fraction, and covariance terms, we have shown that the cloud fraction, cloudy albedo, and cloudy OLR contribute most to the total change in top-of-atmosphere fluxes. The cloudy albedo and cloudy OLR, however, largely offset one another, making the total increase in CRE similar to that driven by cloud fraction changes alone.

We have also done these breakdowns for the total cloud heating effect (direct plus indirect effects), the indirect cloud heating effect, and for changes in sea surface temperature. We focus on high clouds (those whose cloud top pressure is less than 440 hPa). In short, we find ACRE increases CRE in all experiments (though the effect is larger in the limited area domain simulations than in the mock-Walker experiments). The increase in CRE largely comes from the direct interactions of clouds and radiation, while the cloud radiative heating induced stability changes tend to decrease CRE. The cloud changes (albedo, OLR, and fraction) tend to be the dominant factors in determining CRE while the clear-sky and covariance terms tend to be secondary. Warming also leads to a small increase in CRE of about 0–1 W/m^2, owing to changes in clear-sky OLR and cloudy albedo offsetting changes in cloudy-sky OLR. The results we have presented here should apply to other simulations so long as they are capable of simulating realistic anvil clouds. Many models, including the base SAM microphysics, struggle with simulating realistic anvil clouds, hence our modification to the microphysics for this study (as described in section 2).

The total CRE changes are often the result of cancellation between different factors. For example, cloud fraction and albedo changes tend to increase CRE while OLR changes tend to decrease CRE. In other words, not only does ACRE increase the occurrence of high, optically thin clouds, but it also thins and warms those clouds, reducing their albedo while enhancing their OLR. It is worth pointing out that even CRE changes of a few W/m^2 are large percentage changes from the mean because the net cloud radiative effect is close to zero owing to the near cancellation of the shortwave and longwave components of CRE.

The stabilization of the vertical temperature profile tendencies by ACRE, which we show to be the dominant factor in the limited area domains, is mitigated in the mock-Walker experiments. In our warming experiments, the gradient in SST is held fixed, which may exert an unrealistic control on the energy transport from the warm pool to the cold pool. It is unclear whether the balance in cloud fraction enhancement and reduction owing to the cloud-radiation interactions will be maintained if the SST gradients were to be enhanced or reduced.

It is important to note that by using fixed sea surface temperatures, we are limiting our analysis of the cloud-radiation interaction to their within-atmosphere component only. In the real world, the cloud-radiation interactions could also have a profound effect on the surface budget, which is likely to further influence the structure of convection in the tropics. Much of the changes in cloud amount for the direct cloud heating effect occur for high, thin clouds, which do not have much impact on the surface energy budget, so the atmospheric influence is still likely to be the dominant component. The changes in clouds for the indirect cloud heating effect, however, show larger changes for cloud types with high optical depths, which do have a strong surface-forcing component. Future work should be done to quantify how the surface and atmospheric cloud radiative effects work in tandem to alter the tropical circulation patterns.

We have also discussed the potential impacts our results have for understanding cloud feedbacks. Since ACRE is expected to increase in a warmer climate owing to the rising of clouds, we can expect the destabilization of the clouds, the direct cloud heating effect, to increase as well. In our experiments, we find an increase of ACRE per unit cloud fraction of about 1–2% W/m^2/K. Models that are unable to resolve the within-cloud circulations may miss out on this cloud spreading as well as the thinning and warming that accompany it.

Acknowledgments
The authors would like to thank Chris Bretherton and Qiang Fu for useful comments and discussion. Funding for this work was provided by NSF grant AGS-0960497. The model output data used in this study may be obtained upon email request. We also thank our three anonymous reviewers for their comments that helped improve this paper.

References

Ackerman, T. P., K.-N. Liou, F. P. J. Valero, and L. Pfister (1988), Heating rates in tropical anvils, *J. Atmos. Sci.*, *45*(10), 1606–1623.

Bretherton, C. S., P. N. Blossey, and M. Khairoutdinov (2005), An energy-balance analysis of deep convective self-aggregation above uniform SST, *J. Atmos. Sci.*, *62*(12), 4273–4292.

Bretherton, C. S., P. N. Blossey, and M. E. Peters (2006), Interpretation of simple and cloud-resolving simulations of moist convection radiation interaction with a mock-Walker circulation, *Theor. Comput. Fluid Dyn.*, *20*(5–6), 421–442.

Chen, S., and W. R. Cotton (1988), The sensitivity of a simulated extratropical mesoscale convective system to longwave radiation and ice-phase microphysics, *J. Atmos. Sci.*, *45*(24), 3897–3910.

Dinh, T. P., D. R. Durran, and T. P. Ackerman (2010), Maintenance of tropical tropopause layer cirrus, *J. Geophys. Res.*, *115*, D02104, doi: 10.1029/2009JD012735.

Durran, D. R., T. Dinh, M. Ammerman, and T. Ackerman(2009), The mesoscale dynamics of thin tropical tropopause cirrus, *J. Atmos. Sci.*, *66*(9), 2859–2873.

Fu, Q., S. K. Krueger, and K. N. Liou (1995), Interactions of radiation and convection in simulated tropical cloud clusters, *J. Atmos. Sci.*, *52*(9), 1310–1328.

Harrop, B. E., and D. L. Hartmann (2012), Testing the role of radiation in determining tropical cloud top temperature, *J. Clim.*, *25*(17), 5731–5747.

Harrop, B. E., and D. L. Hartmann (2015), The relationship between atmospheric convective radiative effect and net energy transport in the tropical warm pool, *J. Clim.*, *28*(21), 8620–8633.

Hartmann, D., and K. Larson (2002), An important constraint on tropical cloud—Climate feedback, *Geophys. Res. Lett.*, *29*(20), 1951, doi: 10.1029/2002GL015835.

Hartmann, D. L., H. H. Hendon, and R. A. Houze (1984), Some implications of the mesoscale circulations in tropical cloud clusters for large-scale dynamics and climate, *J. Atmos. Sci.*, *41*(1), 113–121.

Hartmann, D. L., L. A. Moy, and Q. Fu (2001), Tropical convection and the energy balance at the top of the atmosphere, *J. Clim.*, *14*(24), 4495–4511.

Iacono, M. J., J. S. Delamere, E. J. Mlawer, M. W. Shephard, S. A. Clough, and W. D. Collins (2008), Radiative forcing by long-lived greenhouse gases: Calculations with the AER radiative transfer models, *J. Geophys. Res.*, *113*, D13103, doi:10.1029/2008JD009944.

Khairoutdinov, M. F., and D. A. Randall (2003), Cloud resolving modeling of the ARM summer 1997 IOP: Model formulation, results, uncertainties, and sensitivities, *J. Atmos. Sci.*, *60*(4), 607–625.

Kristjánsson, J. E., J. M. Edwards, and D. L. Mitchell (2000), Impact of a new scheme for optical properties of ice crystals on climates of two GCMs, *J. Geophys. Res.*, *105*(D8), 10,063–10,079.

Kuang, Z., and D. L. Hartmann (2007), Testing the fixed anvil temperature hypothesis in a cloud-resolving model, *J. Clim.*, *20*(10), 2051–2057.

Lebsock, M. D., C. Kummerow, and G. L. Stephens (2010), An observed tropical oceanic radiative convective cloud feedback, *J. Clim.*, *23*(8), 2065–2078.

Lilly, D. K. (1988), Cirrus outflow dynamics, *J. Atmos. Sci.*, *45*(10), 1594–1605.

Lopez, M. A., D. L. Hartmann, P. N. Blossey, R. Wood, C. S. Bretherton, and T. L. Kubar (2009), A test of the simulation of tropical convective cloudiness by a cloud-resolving model, *J. Clim.*, *22*(11), 2834–2849.

Mace, G. G., S. Benson, and S. Kato (2006), Cloud radiative forcing at the atmospheric radiation measurement program climate research facility: 2. Vertical redistribution of radiant energy by clouds, *J. Geophys. Res.*, *111*, D11S91, doi:10.1029/2005JD005922.

Mlawer, E. J., S. J. Taubman, P. D. Brown, M. J. Iacono, and S. A. Clough (1997), Radiative transfer for inhomogeneous atmospheres: RRTM, a validated correlated-k model for the longwave, *J. Geophys. Res.*, *102*(D14), 16,663–16,682.

Muller, C., and S. Bony (2015), What favors convective aggregation and why?, *Geophys. Res. Lett.*, *42*, 5626–5634, doi:10.1002/2015GL064260.
Muller, C. J., and I. M. Held (2012), Detailed investigation of the self-aggregation of convection in cloud-resolving simulations, *J. Atmos. Sci.*, *69*(8), 2551–2565.
Pierrehumbert, R. (1995), Thermostats, radiator fins, and the local runaway greenhouse, *J. Atmos. Sci.*, *52*(10), 1784–1806.
Powell, S. W., R. A. Houze, A. Kumar, and S. A. McFarlane (2012), Comparison of simulated and observed continental tropical anvil clouds and their radiative heating profiles, *J. Atmos. Sci.*, *69*(9), 2662–2681.
Rossow, W. B., and R. A. Schiffer (1991), ISCCP cloud data products, *Bull. Am. Meteorol. Soc.*, *72*(1), 2–20.
Schiffer, R., and W. Rossow (1983), The International Satellite Cloud Climatology Project (ISCCP)—The first project of the World Climate Research Programme, *Bull. Am. Meteorol. Soc.*, *64*(7), 779–784.
Sherwood, S. C., V. Ramanathan, T. P. Barnett, M. K. Tyree, and E. Roeckner (1994), Response of an atmospheric general circulation model to radiative forcing of tropical clouds, *J. Geophys. Res.*, *99*(D10), 20,829.
Slingo, A., and J. M. Slingo (1988), The response of a general circulation model to cloud longwave radiative forcing. I: Introduction and initial experiments, *Q. J. R. Meteorol. Soc.*, *114*(482), 1027–1062.
Slingo, J. M., and A. Slingo (1991), The response of a general circulation model to cloud longwave radiative forcing. II: Further studies, *Q. J. R. Meteorol. Soc.*, *117*(498), 333–364.
Tian, B., and V. Ramanathan (2003), A simple moist tropical atmosphere model: The role of cloud radiative forcing, *J. Clim.*, *16*(12), 2086–2092.
Tian, B., G. J. Zhang, and V. Ramanathan (2001), Heat balance in the Pacific warm pool atmosphere during TOGA COARE and CEPEX, *J. Clim.*, *14*(8), 1881–1893.
Vecchi, G. A., and B. J. Soden (2007), Global warming and the weakening of the tropical circulation, *J. Clim.*, *20*(17), 4316–4340.
Webster, P. J., and G. L. Stephens (1980), Tropical upper-tropospheric extended clouds: Inferences from winter MONEX, *J. Atmos. Sci.*, *37*(7), 1521–1541.
Wing, A. A., and K. A. Emanuel (2014), Physical mechanisms controlling self-aggregation of convection in idealized numerical modeling simulations, *J. Adv. Model. Earth Syst.*, *6*(1), 59–74.
Wofsy, J., and Z. Kuang (2012), Cloud-resolving model simulations and a simple model of an idealized walker cell, *J. Clim.*, *25*(23), 8090–8107.
Zelinka, M., and D. Hartmann (2010), Why is longwave cloud feedback positive, *J. Geophys. Res.*, *115*, D16117, doi:10.1029/2010JD013817.
Zelinka, M. D., S. A. Klein, and D. L. Hartmann (2012), Computing and partitioning cloud feedbacks using cloud property histograms. Part II: Attribution to changes in cloud amount, altitude, and optical depth, *J. Clim.*, *25*(11), 3736–3754.
Zhang, Y.-C., and W. B. Rossow (1997), Estimating meridional energy transports by the atmospheric and oceanic general circulations using boundary fluxes, *J. Clim.*, *10*(9), 2358–2373.